



# Impact of engine oil volatility and viscosity on blow-by aerosol formation

Kai-Michael Scheiber<sup>1</sup> · Niclas Nowak<sup>2</sup> · Magnus Lukas Lorenz<sup>3</sup> · Jürgen Pfeil<sup>1</sup> · Thomas Koch<sup>1</sup> · Gerhard Kasper<sup>2</sup>

Received: 7 November 2021 / Accepted: 30 January 2022  
© The Author(s) 2022

## Abstract

Particulate emissions from diesel engines are a matter of public concern and continued industrial development. For an internal combustion engine, particles may originate either from the after treatment box or from the crankcase ventilation system. This paper quantifies and discusses particle sources within the crankcase ventilation system of a medium-duty 4-cylinder and a heavy-duty 6-cylinder engine and their dependence on the engine oil parameters viscosity (expressed as Noack number) and HTHS volatility. Crankcase aerosol spectra were measured by an optical particle counter in the size range of 0.3–5 µm. For a few cases data of filter samples downstream the separator unit are discussed for the total blow-by aerosol. Engines were found to behave very similarly with regard to changes in either oil parameter, with volatility generally being the far stronger factor of influence. Total particle mass concentration increased by a factor of up to 5 for a rise in Noack volatility of about 13–25%. The mass concentration downstream of the separator also increases with oil volatility. A variation of HTHS viscosity from 3.5 to 2.6 mPas generated a marginal change in aerosol output by a factor of about 1.2. However, and unexpectedly, the most viscose oil generated the relatively highest particle mass concentrations for both engines.

**Keywords** Crankcase emissions · Blow-by aerosol · PM-emissions · Optical particle counter · OPC · Noack number · Volatility · HTHS value · Viscosity · Oil specification

## 1 Introduction

Emission reduction in the automotive sector has often been driven by legislation, notably Euro VI, which in 2012 imposed particulate emission limits based on total number concentration. Starting with Euro VI-e in 2021, these limits apply also to tests with a portable emission measurement system (PEMS). These tests have also become mandatory under China VI-b regulations. Furthermore, for the scheduled Euro VII emission legislation, the consortium for ultra-low vehicle emissions (CLOVE) proposes to reduce the lower particle size limit for

number concentration measurements from 23 to 10 nm while retaining with the same limit of  $6 \times 10^{11}$  for particles per kWh, which would require an overall reduction of about 70% in particle number concentration [5].

The crankcase of combustion engines is a major source of aerosol particles, beside the combustion vented through the exhaust aftertreatment system. After passing through a particle separator, the remaining, rather fine “blow-by” aerosol is either recirculated to the air intake or directly vented to the environment. Both closed and open crankcase ventilation systems are in current use and have their respective advantages and disadvantages [4]. In either case, however, the additional burden of oily crankcase aerosol represents a problem: In a closed system the particles can cause critical engine components to deteriorate, while in an open system they contribute to the overall emission level included in the emission certification on the test bench or the PEMS measurement procedure on a vehicle.

State-of-the-art passive separators are generally capable of removing super-micron aerosol particles from the blow-by gas, but become much less efficient below about 1 µm [3]. The submicron part of the blow-by aerosol spectrum is,

✉ Kai-Michael Scheiber  
Kai-Michael.Scheiber@kit.edu

Jürgen Pfeil  
Juergen.Pfeil@kit.edu

<sup>1</sup> Institute of Internal Combustion Engines, Karlsruhe Institute of Technology, Karlsruhe, Germany

<sup>2</sup> Institute of Mechanical Process Engineering and Mechanics, Karlsruhe Institute of Technology, Karlsruhe, Germany

<sup>3</sup> Daimler Truck AG, Stuttgart, Germany

therefore, of most concern. According to recent work on the sources of crankcase aerosol, the number size spectrum has two dominant peaks in that size range, one around 200 nm and one around 400 nm [14]. Both are most likely associated with re-condensation of engine oil vapor generated in the hottest regions of the crankcase [11].

Engine oil is a major factor for vehicle performance. Its principal function is of course to lubricate, cool, and clean critical components during operation [7]. Reduced inner friction contributes also to fuel savings and helps to reduce CO<sub>2</sub> emission [15]. A key parameter to that effect is the high-temperature high-shear (HTHS) viscosity of the oil, usually determined at a temperature of 150 °C [1]. A stable HTHS value needs to be maintained as long as possible, despite the accumulation of soot and unburned fuel, to maximize oil change intervals. The oil formulation is furthermore critical in minimizing the consumption of engine oil, driven by oil transport to the combustion chamber as well as evaporation at elevated temperatures. Oil evaporation is characterized by the Noack volatility, defined as the percentage of oil mass loss during 60 min at 250 °C [2].

The relevance of oil volatility for aerosol production, and hence of the oil temperature within an engine, especially of local extremes in so-called hot-spots, has already been pointed out [8]. However, the impact of key parameters such as HTHS viscosity and Noack volatility on aerosol production has never been investigated exhaustively.

This paper investigates their effects on aerosol formation in the crankcase environment. It does so on the basis of five different oils in combination with two commercial diesel engines of differing designs and applications, operated across a wide range of loads and speeds. Aerosol characterization generally focusses on the particle size spectrum between 0.3 and 5 µm, where particle mass and number concentrations were recorded continually by an optical particle counter (OPC). Note that all size-spectrometric aerosol characterization was done before any separation unit, to obtain actual engine emissions rather than the characteristics of the separator. A few additional measurements were conducted gravimetrically to obtain total emissions downstream the separation unit.

## 2 Materials and methods

### 2.1 Aerosol sampling and characterization

Crankcase aerosols were characterized by an OPC of the type Palas Promo 2000 H in combination with the Palas Welas 2070 HP sensor. The device measures the size of particles in the range of nominally 0.3 µm to 10 µm on the basis of their scattered light intensity and sorts them into 32 size bins per decade of logarithmically equal width. It

determines the entire spectrum with a temporal resolution of 1 Hz. The OPC was operated with the built-in calibration for oil (refractive index 1.47) to ensure a reliable determination of the physical size of oil droplets, and thus also a relatively accurate conversion of drop diameter to drop volume required for conversions from number to mass concentration.

The OPC has a nominal upper concentration limit of 10<sup>6</sup> cm<sup>-3</sup>, but in fact requires an elaborate sampling two-stage dilution system to maintain total concentrations well below that nominal limit. Dilution was done with particle free air. The sampling system was designed also to avoid various kinds of measuring artifacts typical of mixtures of oil vapor and aerosol emerging from the crankcase of a combustion engine. A detailed description including the precautions taken to ensure reliable results is given by Nowak et al. [10].

For both engine studies, aerosols were extracted at equivalent positions in the blow-by path inside the valve covers just before the blow-by flow enters the crankcase ventilation system and separators. This sampling location was shown in previous studies to give stable and representative results [9] for a sampling time of 5 min. Sampling was done with a sharp-edged 8-mm probe inserted vertically into the valve cover from above, so that the probe tip faced the oncoming air flow field between the valve trains. Sampling and dilution systems were similar but not identical for the two engines used in this study. This will have some effects on the concentration of larger particles, above about 5 µm which may differ between engines. However, engine comparisons were not the objective of the current study. Data sets for parameter variations for a given engine will be consistent.

In addition, data for the total blow-by aerosol concentration downstream of the separator will be reported for a few cases. These were obtained with a BAF 7000 filter system (Möhwald GmbH) according to [6]. The device includes a wall flow trap to ensure only the aerosol reaches the filter. Further downstream this aerosol loads a filter by two layers of pre-conditioned (at 110 °C) highly efficient glass fiber media.

### 2.2 Engine properties

The study was conducted on two diesel engines, a medium-duty 4-cylinder engine produced in series by Daimler Truck AG (designated in the following as OM934) and a heavy-duty 6-cylinder prototype engine (designated in the following as OM471P). The medium-duty engine is geared toward distribution tasks on the Atego™ line, the heavy-duty engine for long-haul tasks on the Actros™ line. Both engines operate within EURO VI guidelines.

According to Table 1 the engines differ first and foremost in their displacement and, consequently, also in related characteristics. Maximum BMEP, peak firing pressures and

power density are also somewhat higher for the heavy-duty engine (OM471P). This tends to increase aerosol source strengths via such factors as the aerosol slippage across piston rings or internal hot-spot temperatures. One may, therefore, expect the absolute aerosol output of the heavy-duty OM471P engine to be generally higher than that of the medium-duty OM934.

However, comparisons of *absolute* aerosol output between engines are of lesser interest for this study than the *relative effect* of a change in oil properties for a given engine. Also, engine design should not dominate over the influence of the oil. It was, therefore, necessary to ensure that the aerosol production mechanisms inside the crankcase remain basically the same for both engines. In this regard, the shape of the aerosol particle size spectrum (Fig. 1), and in particular the location of characteristic peaks is a good indicator, as was shown during previous studies [10, 12]. The figure compares crankcase aerosol particle size spectra for the OM934 and the OM471P with measurements on the same engine family (4 engines including the OM934) from an earlier study [14]. The range of these earlier data is represented as a gray scatter band. To bring out their shape rather than absolute differences, each PSD is normalized by its total particle concentration,  $C_n^{tot}$  or  $C_m^{tot}$ , in the size range of 0.4 to 1.3  $\mu\text{m}$ . Note that these PSD are all closely grouped together and very similar in shape, both for the number concentration-based PSD (Fig. 1a) and the mass concentration-based PSD (Fig. 1b).

The PSDs of the OM471P and OM934 are thus well within the range of other medium- and heavy-duty engines. The underlying aerosol formation processes are, therefore, essentially the same. Conversely, we may, therefore, infer that any significant changes in spectral shape would have to be due to the influence of a particular oil.

**Table 1** Selected engine characteristics

	OM934	OM471P
Number of cylinders	4	6
Total displacement/L	5.1	12.8
Max. blow-by flow/L/min	80	200
Max. torque/Nm @ speed/rpm	900 1200	2600 1100
Max. power/kW @ speed/rpm	170 2200	390 1600
Max. BMEP/bar	21	25+
Peak firing pressure/bar	210	230+
First oil fill/L	20	45
Max. oil flow/L/min	110	230
Piston material	Aluminum	Steel
Turbocharger	Dual stage	Single stage

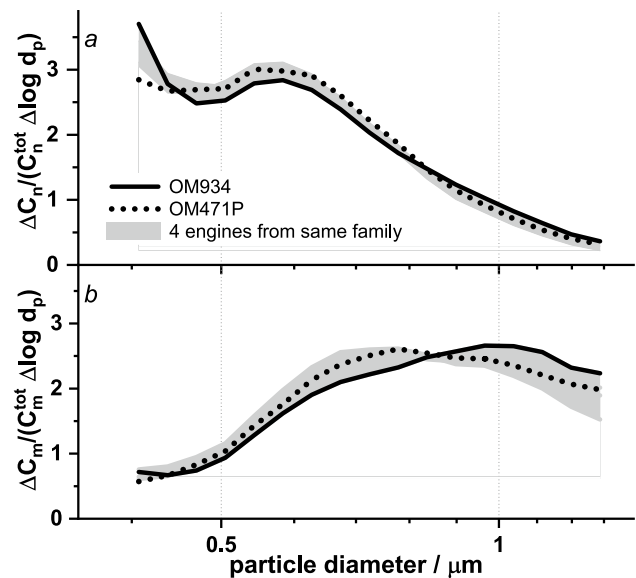


**Fig. 1** Comparison of crankcase aerosol PSD by number (a) and mass (b) for several engines, including data for four engines from earlier study [14]. These earlier data are represented in terms of a scatter band.  $\Delta\log dp$  represents the logarithmic width of particle size classes used by the OPC

### 2.3 Engine oil properties

Oil aerosol in the crankcase of combustion engines can form either by mechanical processes such as jet or rotary atomization, or by condensation of supersaturated hydrocarbon vapors upon cool-down. The two most important oil properties governing these mechanisms are the viscosity and the saturation vapor pressure, both of which are strong functions of temperature. (The saturation vapor pressure of commercial oils rises by about one order of magnitude for each temperature increment of 30 to 40  $^{\circ}\text{C}$ .) On the one hand, a more volatile oil is expected to boost the blow-by aerosol concentration because hot-spots generate more oil vapor. On the other hand, decreasing oil viscosities are also expected to boost aerosol generation by oil jet break-up because the state (described by the Ohnesorge and Reynolds number) is shifted towards the atomization regime in the Ohnesorge diagram [13].

The five engine oils selected for the study (Table 2) fall into two groups: three oils with different saturation vapor concentrations and volatility parameters but comparable viscosity, and three oils with different viscosities but comparable volatility. Oils denoted as A, B, and C are custom formulations because commercial products with a suitable spread in volatility parameters but almost constant viscosity could not be found.

Oil viscosity data such as HTHS or kinematic viscosity are widely available in the literature. However, with regard to vapor pressure or volatility, only Noack volatilities are

readily available. In addition, saturation vapor concentrations would also be helpful to estimate relative aerosol mass production rates for different oils. Since these are not readily available in the open literature, they were determined by cold trap experiments for the customized oils used in this study. The details of this method are described by Nowak et al. [11].

## 2.4 Design of the study

The current study focusses on the impact of engine oil properties on crankcase aerosol emissions, and specifically of oil volatility (based on the NOACK number) and viscosity (based on HTHS value) across a broad range of engine states (see Table 3). Three oils with a sufficient spread in respective parameter values were chosen for each set of comparisons as indicated in Table 2. The oil viscosity was varied from an HTHS value of 3.5–2.6 mPas for oils with very

similar volatilities; the oil volatility in the range of Noack numbers of 13–25% with oils of nearly the same kinematic viscosity. The respective impact of those two oil parameters was investigated for both engines at three engine operating cases each.

Engines were run with the same or very similar test-bench boundary conditions wherever possible: either a constant coolant inlet temperature of 90 °C or a constant engine oil temperature of 115 °C. The only exception are the measurements of volatility vs. load and speed. These had to be carried out with the OM471P at constant engine oil temperature (vs. the OM934 at constant coolant inlet temperature) because it was run on a different test bench. Comparative measurements (Fig. 2) showed, however, that this affected only the absolute aerosol output of the OM471P as a function of oil properties, not relative changes in PSD shape.

Figure 2 shows two PSD from the same OM471P engine, operated once with the coolant inlet temperature maintained

**Table 2** Key engine oil characteristics

	*R6 LME	*Ultra E Plus	Oil A	Oil B	Oil C
SAE viscosity	5 W-30	5 W-30	0 W-20	0 W-20	0 W-20
Kin. viscosity					
@ 40 °C/mm <sup>2</sup> /s	67	51	42	44	44
@ 100 °C/mm <sup>2</sup> /s	12	9	8	8	8
Viscosity index/-	178	170	166	156	156
HTHS class @ 150 °C/mPa s	<b>3.5</b>	<b>2.9</b>	<b>2.6</b>	2.6	2.6
Noack volatility/%	10	10	<b>13</b>	<b>20</b>	<b>25</b>
Saturation vapor concentration**@ 120 °C/mg/m <sup>3</sup>	120	–	140	380	3600
Density /kg/m <sup>3</sup> @ 15 °C	845	840	841	839	839
Mercedes Benz specifications for operating fluids (MB BeVo)	225.18	225.21	–	–	–

\*Shell Rimula

\*\*Measured for fresh oil

**Table 3** Engine operating strategy selected for oil property comparisons

	NOACK/% 13   20   25	HTHS/mPa s 3.5   2.9   2.6
Low-end torque point at full load	<b>OM934</b> <sup>2</sup> at 1200 rpm, 21 bar <b>OM471P</b> <sup>2</sup> at 1100 rpm, 25 bar	<b>OM934</b> <sup>1</sup> at 1200 rpm, 21 bar <b>OM471P</b> <sup>1</sup> at 1100 rpm 25 bar
Load	<b>OM934</b> <sup>1</sup> at 1200 rpm:	<b>OM 934</b> <sup>1</sup> at 1200 rpm:
Variation	0/ 5/ 15/ 21	0/ 5/ 15/ 21
BMEP/bar	<b>OM471P</b> <sup>2</sup> at 1100 rpm: 5/ 12/ 19/ 25	<b>OM471P</b> <sup>1</sup> at 1100 rpm: 5/ 12/ 19/ 25
Speed	<b>OM934</b> <sup>1</sup> :	<b>OM934</b> <sup>2</sup> :
Variation	1200/ 1600/ 1800/ 2200	1200/ 1600 /1800 /2200
rev/rpm	<b>OM471</b> <sup>2</sup> :	<b>OM471</b> <sup>2</sup> :
At full load	1000/ 1100/ 1200/ 1400/ 1600	1000/ 1100/ 1200/ 1400/ 1600

1: Regulated coolant inlet temperature 90 °C

2: Regulated engine oil temperature 115 °C

at 90 °C (blue) and once with the engine bulk oil temperature maintained at 115 °C (red). The PSDs are normalized by the total concentration at constant engine bulk oil temperature. Evidently, the distributions differ in their absolute level but retain the same shape and peak positions. Comparisons between engines regarding the relative are thus permitted, even when the engine boundary conditions differ.

### 3 Results

In the following, data are first presented and discussed in terms of the full PSD in the size range of 0.3 to 5  $\mu\text{m}$ , obtained at one engine condition (low-end torque, defined as maximum engine load at minimum speed). These data will be analyzed to ascertain that different types of oil do not lead to significant changes in PSD shape, which would imply changes in aerosol generating mechanisms. After that, results different engine loads and speeds will be presented and discussed in terms of total concentration (based on number as well as mass) in that size range. Kinematic viscosities, expressed as HTHS, as well as oil volatility, expressed as Noack number, were each varied in three steps for both the medium and heavy-duty engine. Oil properties and engine operating data can be found in Tables 2 and 3, respectively.

#### 3.1 Impact of viscosity and volatility on the shape of the blow-by aerosol particle size distribution

Figure 3 shows the impact of changes in oil volatility or viscosity on the PSD of the oil aerosol, measured at the low-end

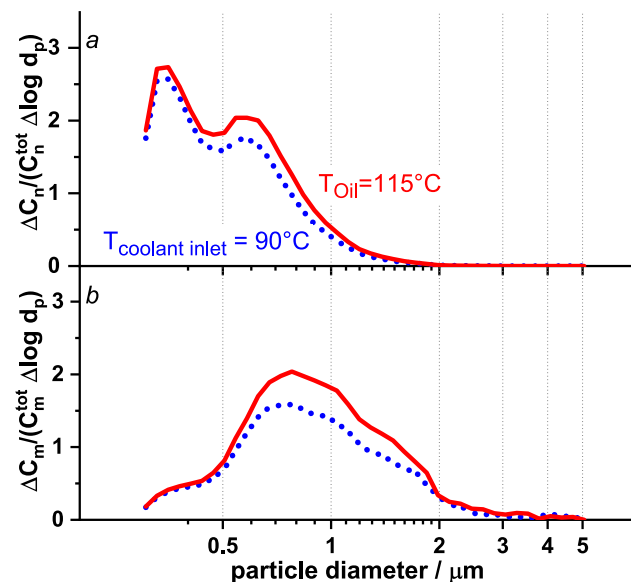


**Fig. 2** Influence of test-bench boundary conditions on the PSD of number (a) and mass (b) of the OM471P operated at 1100 rpm and full load

torque operation point. PSDs are represented on the basis of both particle number (plots a and c) and mass concentration (plots b and d). PSDs for the OM934 are depicted as solid lines, for the OM471P as dotted lines. Each PSD is normalized by its respective total concentration in the size range of 0.3 to 5  $\mu\text{m}$ . Curves for volatilities and viscosities are color-coded from the highest (red) to lowest (blue) values.

The *absolute* aerosol output varies widely, both between engines and for different oil volatilities as will be discussed in the following subchapters. However, with regard to *shape*, the PSDs are all multimodal and quite similar, both across the range of oil properties and also between engines. According to Fig. 3, the PSDs are all multimodal, which is best seen in the mass-based PSD. Peaks are characteristically located around 0.8–0.9  $\mu\text{m}$  for the submicron and around 2  $\mu\text{m}$  for the super-micron spectrum. For the number-based PSD the peak at 2  $\mu\text{m}$  is only weakly expressed as there are high amounts of submicron particles over all variations. However, the heavy-duty engine tends to produce slightly more super-micron particles than the medium-duty engine in relation to the overall particle spectrum covered by the measurements (0.3 to 5  $\mu\text{m}$ ).

With increasing volatility, the 2- $\mu\text{m}$  peak in the mass-based spectrum becomes very pronounced for the heavy-duty engine, while at lower volatilities it tends to disappear. For the range of viscosities covered in these experiments, the heavy-duty engine produces mainly fine aerosols with a dominant peak around 0.8  $\mu\text{m}$ , while the spectra of the medium-duty engine contain finer and coarser particles in roughly equal proportion.

These are indications for multiple aerosol formation mechanisms inside each engine, but also that the mechanisms are essentially the same for both engines. Engines appear to differ mainly in proportions and quantity of aerosols produced.

With increasing oil volatility, the PSDs are generally shifted to the right, toward larger particle diameters. This trend is undoubtedly due to the availability of more oil vapor that condenses on pre-existing particles during cool-down [11], thereby increasing their diameters. The diameter increase affects particles of all sizes, including those originally below the detection limit of the OPC (approx. 0.3  $\mu\text{m}$ ), which can now move cross the detection threshold into the lowest OPC size classes. This is nicely illustrated in the transition of the number PSDs with increasing volatility. When raising the volatility from Noack value 13 to 20%, only the number concentration in the range  $< 0.7 \mu\text{m}$  rises for both engines. From 20 to 25% the entire distribution moves to the right and the impact is seen especially for the mass concentration.

Absolute concentrations can of course not be deduced from the normalized PSD in Fig. 3. It should be mentioned, however, that total concentrations also increase with oil

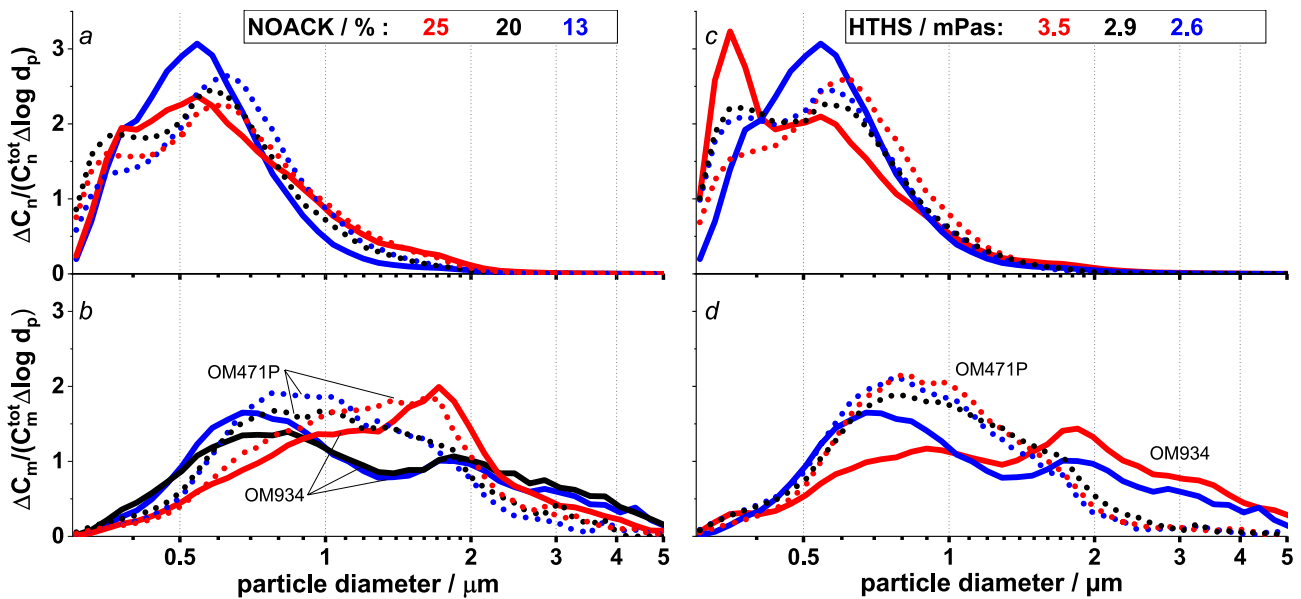


**Fig. 3** Impact of oil volatility and viscosity on aerosol particle size distributions based on number (a, c) and mass (b, d) concentration. Measurements are at the low-end torque engine operation point. PSD

volatility. The mass concentration increase is 20–30% (OM471P vs. OM934) from the lowest to the intermediate volatility (blue to black curves), and by another 110–180% (OM471P vs. OM934) from the black to the red curves. The following sections will give a more complete discussion of concentration dependence across a range of engine parameters.

### 3.2 Impact of volatility and viscosity on the total aerosol output as a function of engine load at constant speed

Figure 4 describes the impact on the total aerosol concentration of varying oil volatilities and kinetic viscosities across a range of engine loads. Engine loads are expressed as BMEP, a parameter which represents the engine load independent of engine size. As before, aerosol concentrations are represented both by particle number ( $C_n$ ) and by particle mass ( $C_m$ ). Concentrations are always normalized with regard to the maximum total concentration of the higher emitting engine, in each case the OM471P engine. This is denoted as  $C_n^{\max}$  or  $C_m^{\max}$ .

According to Fig. 4, the two engines differ by up to an order of magnitude in absolute crankcase aerosol output. In view of their substantially different displacement volumes, different power output, different peak pressures etc., this was to be expected. For both engines, particle emission levels increase exponentially with BMEP by factors between about 3.5 and 5. The exponential dependence is consistent with earlier observations by Scheiber et al. [14].

are normalized by the, respectively, total concentration in that size range (viscosity = 2.6 mPa s for all volatility variations, and volatility = Noack 10–13% for all viscosity variations)

Of greater interest than the similarities between them are the respective engine responses to a change in oil properties. According to Fig. 4, a volatility increase from Noack 13% to Noack 25% increases the aerosol mass concentration of either engine by a factor of roughly 3 across the range of operating conditions, due to the attendant increase in saturation vapor concentration. According to Table 2 that increase is roughly threefold from 13 to 20%, and a further tenfold from 20 to 25%. When comparing the increase in emission levels (3-fold) with that of the vapor concentrations (approx. 25-fold), it appears that only a fraction of the vapor generated in engine hot-spots can actually contribute to condensational growth of particles. The chief reason for this apparent discrepancy lies in the increased and rather dominant vapor losses to the inner engine walls while the aerosol is transported out of the engine. These walls present a far larger surface area and condensation sink than the aerosol. This is discussed in more detail by Nowak et al. [11].

It is also worth noting that Noack numbers change by a factor of about 2 for the entire range of volatilities covered by the experiment, while vapor pressures increase approx. 25-fold. The measured increase in total aerosol production (about 3-fold), therefore, scales more closely with the Noack number than with total available vapor concentration. The Noack number may be a poor measure of saturation vapor concentrations, but it seems to be a better indicator of relative aerosol production.

The impact of changes in oil viscosity are presented in the right-hand side of Fig. 4. HTHS viscosities, the parameter used in this diagram, are a high-temperature measure for the

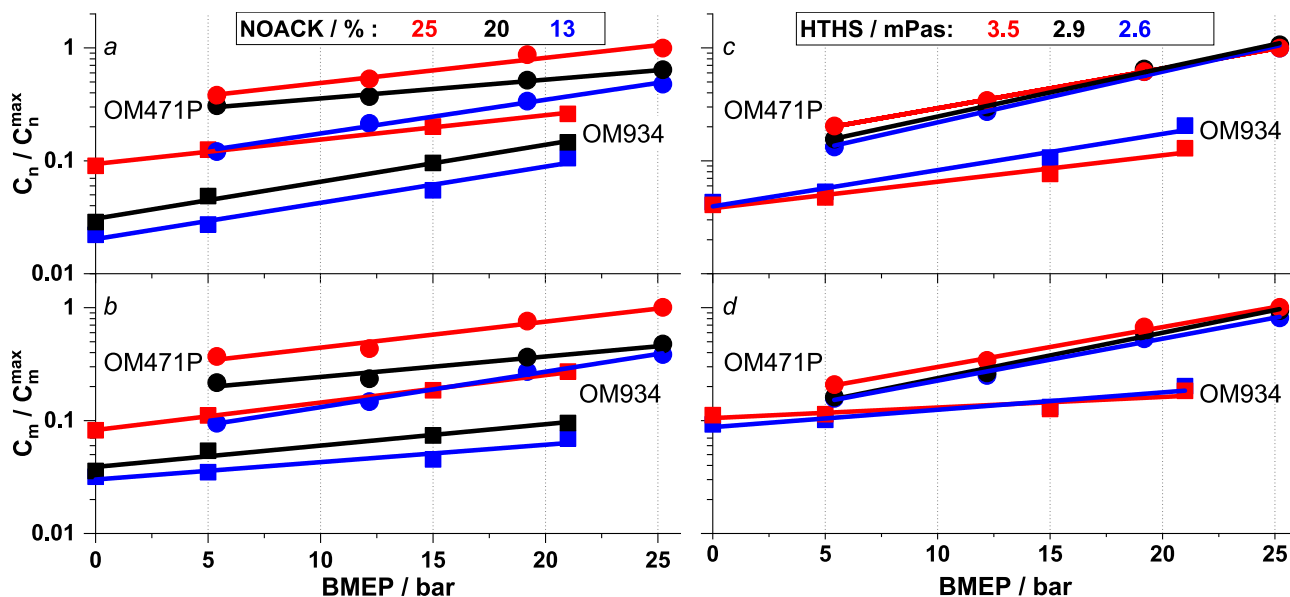


**Fig. 4** Impact of volatility and viscosity on total aerosol concentration by number (a, c) and mass (b, d) as a function of engine load (expressed as BMEP) at a fixed engine speed of 1100 and 1200 rpm,

respectively. All concentrations are relative the maximum total concentration of the OM471P. Regression lines are exponential fit functions

relative degree of mechanical dispersion and atomization of individual oils.

By contrast, the spread in emission levels is much smaller than those caused by a change in volatility. Although HTHS values were varied by a factor of about 1.5. For a wide range of engine loads the spread is insignificant, especially for the OM471P. Only the OM934 shows an increase by roughly a factor of 2 from the highest to the lowest viscosity, and only at the highest load levels in combination with a low engine speed.

### 3.3 Impact of volatility and viscosity on the total aerosol output as a function of engine speed at full load

Figure 5 shows the impact of volatility (left) and viscosity (right) on crankcase aerosol emissions along the full-load curve. The volatility is expressed as Noack, the viscosity as HTHS.

Evidently, the heavy-duty engine is always the higher emitter of the two engines. This has been expected because it runs at a higher peak pressure and also somewhat hotter, due to its piston material. According to the figure, mass concentrations of the OM471P lie between 2 and 4 times above those of the OM934.

More importantly, one sees that the total aerosol output of either engine increases significantly with engine oil volatility while the influence of the HTHS viscosity is much weaker across the entire range of speeds.

The medium-duty engine reacts differently to a change in engine speed than the heavy-duty engine. OM934 mass concentrations tend to rise with rpm (albeit slowly in case of the viscosity), while OM471P concentrations tend to be flat or decrease. These opposing behaviors along the speed axis may be due to differences in engine layout: For one, the medium-duty engine delivers its peak torque in a wide speed range while the heavy-duty engine is designed for a narrow peak torque range at low engine speed around 1100 rpm.

Thermodynamic conditions favorable for aerosol production are, therefore, highest at opposing ends of the speed axis. Interestingly, the effect is most pronounced for the mass-based data. While mass concentrations decrease toward the right for the OM471P, number concentrations continue to rise. Apparently, the particles become more and finer, but carry less mass in total.

An additional difference between engines concerns their turbocharger layouts. In contrast to the OM471P, the OM934 is equipped with a dual-stage unit. Hence there are more shafts and bearings to be supplied by an oil pump linked to engine speed. Also, the exhaust gas temperatures rise towards the nominal power at 2200 rpm. The role of the turbocharger can be considerable for some engines, as already pointed out in earlier work [9], where a contribution up to 30% of the total mass concentration reported.

In sum, both factors help to explain why the crankcase aerosol contribution of the OM934 runs counter-current to that of the OM471P.

### 3.4 Total aerosol output vs. volatility, measured before and after a mist separator

So far, the results have shown that—between the two oil parameters investigated here—the volatility is the dominant factor for aerosol production *within* the engine crankcase. The question now arises, how this increase affects emissions *after* the built-in mist separator. This will be discussed for the case of the heavy-duty OM471P engine.

Figure 6a presents measurements of total aerosol mass concentration before and after the separator for the three oils used throughout this study. The measurements were made at the low-end torque point, i.e. for maximum power. The mass concentration after the separator is based on filter samples (hence with an undefined size range) the concentration before the separator uses the OPC data in the size range of 0.3 to 5  $\mu\text{m}$ . For comparison, both data sets were normalized by their respective minimum concentrations at Noack 13%.

Figure 6a shows that the non-linear and rather steep increase in mass emission with oil volatility coming from the OM471P engine is passed on to the downstream side of the separator. The proportions are not exactly the same, possibly due to the difference in sampling and measurement methods. (Note also, that these are not absolute levels but relative changes due to variation in oil viscosity) Filter samples may contain some larger drops excluded from the OPC data. However, even this semi-quantitative comparison is revealing.

For an interpretation, it is useful to return to the behavior of the upstream aerosol. Figure 6b shows the corresponding particle size distributions in the size range used also for the previous figures, i.e. 0.3 to 5  $\mu\text{m}$ . To bring out

the increase with Noack number, all PSDs were normalized by the total mass concentration of the OM471P at Noack 25% (This is a different representation from Fig. 2, where each PSD was normalized by its own total concentration). The OM934 data were added for completeness.

Figure 6b not only reflects the increase in total mass with volatility, but it shows that this rise is centered around fine particles below about 2  $\mu\text{m}$  in the size, where most inertial separators begin to lose their efficiency. This may help to explain why the increase in fine aerosol concentration is passed on disproportionately to the downstream side. It also emphasizes the effect of low-volatility oils on crankcase emissions.

## 4 Summary and conclusions

The paper discusses the impact of two key engine oil parameters on blow-by aerosol formation, namely the oil viscosity expressed as HTHS (high-temperature high-shear viscosity) value and the oil volatility expressed by Noack number.

The investigation is based on two engines designated for commercial vehicles by Daimler Truck AG: a medium-duty 4-cylinder engine produced in series, and a heavy-duty 6-cylinder prototype engine. Test were performed on benches located at the KIT and Daimler. Measurements were made for low-end torque operation, and across a range of loads and speeds, using the same or very similar boundary conditions for both engines.

The experimental range of oil parameters was covered with five engine oils that fall into two groups: three oils with different saturation vapor concentrations and volatility

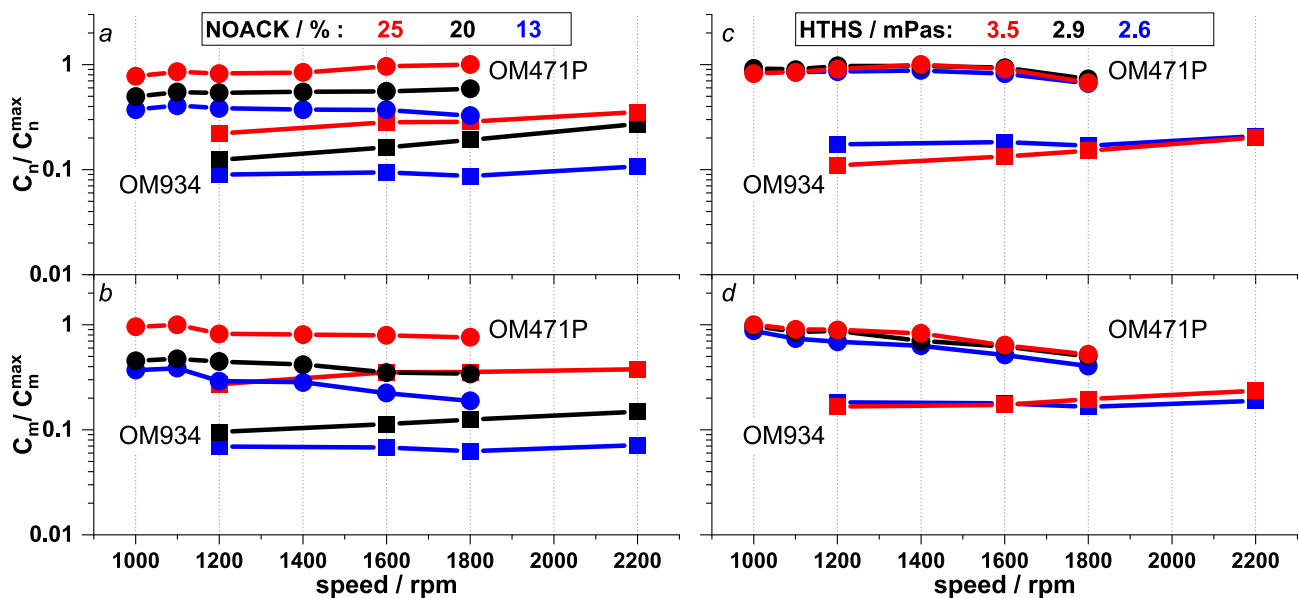


**Fig. 5** Impact of volatility and viscosity on total aerosol concentrations by number (a, c) and mass (b, d) as a function of engine speed at full load. All concentrations are relative the maximum total concentration of the OM471P

indices (Noack number of 13 to 20 to 25%) but similar viscosities, and three oils with different viscosities (HTHS value of 2.6 to 2.9 to 3.5 mPas) but comparable volatilities. The three engine oils required to vary the Noack number were custom formulated because commercial products with a suitable parameter spread could not be found. For these custom oils the required vapor concentration vs. temperature data were determined by cold trap experiments at KIT [11].

Crankcase aerosols were characterized by an optical particle counter (OPC) in the size range of 0.3 to 5  $\mu\text{m}$  and represented either as particle size distributions (PSD) by both number and mass, or as total concentrations in that range. For both engines the sampling was extracted at equivalent positions in the blow-by path inside the valve covers just before the blow-by flow enters the crankcase ventilation and separator system.

For all five engine oils and for the entire range of engine operation, PSDs varied in absolute level but remained very similar in shape. In particular they retained their bimodal shape with peaks around 0.8–0.9  $\mu\text{m}$  and 2  $\mu\text{m}$ . This bimodal shape was also observed for both engines, although with differences in absolute levels. Hence, we conclude that aerosol formation mechanisms remained basically the same for both engines and across their respective ranges of engine operation.

The crankcase aerosol characteristics were discussed with regard to their dependence on oil properties (viscosity and volatility) as well as their dependence on engine operating parameters (notably load and speed).

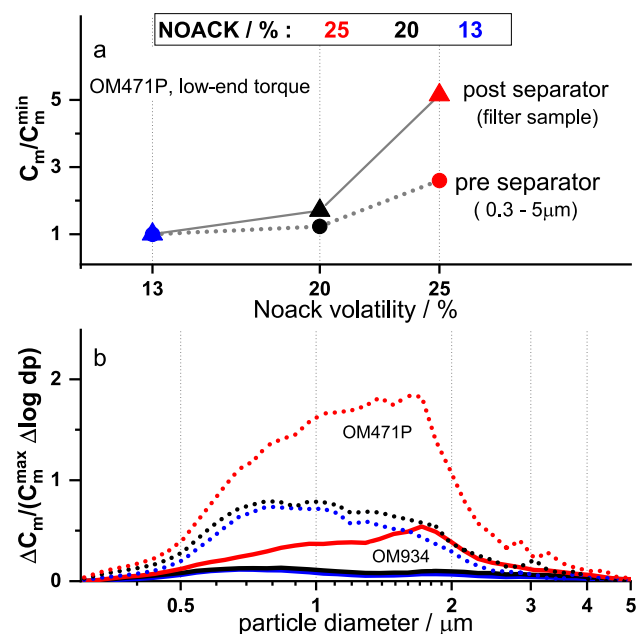


**Fig. 6** **a** Changes in total mass emission and PSD with volatility relative to the emission at Noack 13% for the OM471P engine in low-end torque operation, measured before and after an oil mist separator. **b** PSDs normalized by the total mass concentration of the OM471P at Noack 25%

With regard to oil properties the data consistently showed a relative strong dependence on volatility, but a weak (or even very weak) dependence on viscosity.

An increase of volatility from Noack 13% to Noack 25% (a factor of roughly 2) increased the aerosol mass concentration of either engine by a factor of roughly 3 across the range of operating conditions, due to the attendant, nearly 30-fold increase in saturation vapor concentration. Thus, only a fraction of the generated vapor mass is involved in aerosol formation and growth while most vapor condenses on system walls, consistent with earlier work [11]. The Noack number appears to be a better estimator for the influence of volatility on aerosol formation, than the actual saturation vapor concentration.

It was also found that the increase in aerosol generation with volatility occurred in the particle size range below about 2  $\mu\text{m}$ , a size range where the efficiency of mist separators begins to drop. This may explain why, for the heavy-duty engine, the increase in crankcase aerosol mass concentration was reflected in a proportionate increase in aerosol downstream of the oil mist separator.

A roughly 1.5-fold variation in viscosity between HTHS 2.6 and 3.5 mPas typically lead to changes in aerosol load ranging from marginal to a factor of about 1.2, except under specific engine conditions. Surprisingly, the most viscous oil often led to the highest aerosol load. There is no straightforward explanation for this behavior, which may have to do with specific additives.

With regard to engine parameters, the strongest influence on the crankcase aerosol was the engine load. During engine load step operation, the thermodynamic conditions as well as the components stress rise continually, leading to an exponential increase in aerosol mass concentration with BMEP, for all oils and both engines. The exponential dependence is consistent with earlier work [14].

Speeding up either engine at full load had a far smaller impact on crankcase aerosol production than the load variation. In addition, there were certain, small, engine specific effects having to do with the speed at which an engine operates under full load and the turbocharger layout. The above-mentioned effects of viscosity and volatility were, however, preserved across the full range of engine speeds. On an absolute level, the two engines differed by a factor of up to 6 times in aerosol production. In view of their substantially different displacement volumes, absolute power, etc. this was, however, not surprising.

In sum, one of the most effective in-engine reduction measures for crankcase emission is the choice of an engine oils with low volatility. This aspect should be considered as an additional criterion for selecting an engine oil.

Table 4 lists the notations.

**Table 4** Notations

Symbol	Unit	Physical quantity, description
BMEP	Bar	Brake mean effective pressure
CLOVE		Consortium for ultra-low vehicle emissions
HTHS	mPas	High temperature high-shear viscosity
NOACK	%	Mass loss after NOACK volatility test
OPC		Optical particle counter
PEMS		Portable emissions measurement system
PSD		Particle size distribution
PM		Particle matter
PN		Particle number
$C_n$	$\#/cm^3$	Particle number concentration
$\Delta C_n$	$\#/cm^3$	Particle number concentration per size bin
$C_n^{tot}$	$\#/cm^3$	Total particle number concentration
$C_n^{max}$	$\#/cm^3$	Maximum particle number concentration at test series
$C_m$	$mg/m^3$	Particle mass concentration
$\Delta C_m$	$mg/m^3$	Particle mass concentration per size bin
$C_m^{tot}$	$mg/m^3$	Total particle mass concentration
$C_m^{max}$	$mg/m^3$	Maximum particle mass concentration at test series
$C_m^{min}$	$mg/m^3$	Minimum particle mass concentration at test series
$dp$	$\mu m$	Particle diameter

**Acknowledgements** The authors gratefully acknowledge financial and technical support from Daimler Truck AG, Liebherr-International S.A., MAHLE GmbH, MTU Friedrichshafen GmbH, and UT99 AG, the members of the Engine Crankcase Emissions Consortium at the KIT.

**Funding** Open Access funding enabled and organized by Projekt DEAL.

**Open Access** This article is licensed under a Creative Commons Attribution 4.0 International License, which permits use, sharing, adaptation, distribution and reproduction in any medium or format, as long as you give appropriate credit to the original author(s) and the source, provide a link to the Creative Commons licence, and indicate if changes were made. The images or other third party material in this article are included in the article's Creative Commons licence, unless indicated otherwise in a credit line to the material. If material is not included in the article's Creative Commons licence and your intended use is not permitted by statutory regulation or exceeds the permitted use, you will need to obtain permission directly from the copyright holder. To view a copy of this licence, visit <http://creativecommons.org/licenses/by/4.0/>.

## References

- ASTM International: Test Method for Measuring Apparent Viscosity at High-Temperature and High-Shear Rate by Multicell Capillary Viscometer, 5481st edn. ASTM International, West Conshohocken, PA **75.100** (2021)
- Deutsches Institut für Normung e. V.: Prüfung von Mineralölerzeugnissen – Bestimmung des Verdampfungsverlustes. Teil 1: Verfahren nach Noack. Beuth Verlag GmbH **75.080**(51581-1) (2011-09-00)
- Golkarfard, V., Subramaniam, R., Broughton, J., King, A., Mullins, B.: Comparative performance of 12 crankcase oil mist separators. SAE Int. J. Engines **12**(1), 5–14 (2019). <https://doi.org/10.4271/03-12-01-0001>
- Greuter, E., Zima, S., Hoffmann, W.: Motorschäden. Schäden an Verbrennungsmotoren und deren Ursachen, 4th edn. Vogel-Fachbuch. Vogel, Würzburg (2011)
- Hausberger, S., Weller, K., Ehrly, M.: Scenarios for HDVs. Summary Emission Limits and Test Conditions Status 08.04.2021. Consortium for ultra Low Vehicle Emissions. <https://circabc.europa.eu/sd/a/b706ffba-f863-4d23-809d-20d9f18ecba4/AGVE>. Accessed 17 Jan 2022
- International Organization for Standardization: Road vehicles - Aerosol separator performance test for internal combustion engines. Part 1: General **43.060.20**(17536-1) (2015-12-00)
- Küntschler, V., Hoffmann, W.: Kraftfahrzeugmotoren. Auslegung und Konstruktion, 5th edn. Vogel Buchverlag, s.l. (2015)
- Lensch-Franzen, C., Gohl, M., Scholl, P., Paoloni, F.: Impact of engine lubricant volatility on oil and particle emissions. MTZ Worldw **80**(9), 44–53 (2019). <https://doi.org/10.1007/s38313-019-0087-z>
- Lorenz, M.L., Koch, T., Kasper, G., Pfeil, J., Nowak, N.: Origin and separation of submicron oil aerosol particles in the blow-by of a heavy-duty diesel engine. SAE Int. J. Engines (2020). <https://doi.org/10.4271/03-13-03-0024>
- Nowak, N., Scheiber, K., Pfeil, J., Meyer, J., Dittler, A., Koch, T., Kasper, G.: Sampling and conditioning of engine blow-by aerosols for representative measurements by optical particle counters. J. Aerosol Sci. **148**, 105612 (2020). <https://doi.org/10.1016/j.jaerosci.2020.105612>
- Nowak, N., Sinn, T., Scheiber, K., Straube, C., Pfeil, J., Meyer, J., Koch, T., Kasper, G., Dittler, A.: On aerosol formation by condensation of oil vapor in the crankcase of combustion engines.

- Aerosol Sci. Technol. (2021). <https://doi.org/10.1080/02786826.2021.1976720>
12. Nowak, N., Scheiber, K., Stieler, C., Heller, M.T., Pfeil, J., Koch, T., Kasper, G.: On Blow-by Aerosol Sources in a Single-Cylinder Crankcase Environment. In: ASME 2021 Internal Combustion Engine Division Fall Technical Conference. ASME 2021 Internal Combustion Engine Division Fall Technical Conference, Virtual, Online, 13.10.2021 - 15.10.2021. American Society of Mechanical Engineers (10132021). <https://doi.org/10.1115/ICEF2021-70947>
  13. Ohnesorge, W.V.: Die Bildung von Tropfen an Düsen und die Auflösung flüssiger Strahlen. *Z. Angew. Math. Mech.* **16**(6), 355–358 (1936). <https://doi.org/10.1002/zamm.19360160611>
  14. Scheiber, K.-M., Nowak, N., Lorenz, M.L., Pfeil, J., Koch, T., Kasper, G.: Comparison of four diesel engines with regard to blow-by aerosol properties as a basis for reduction strategies based on engine design and operation. *Automot. Engine Technol.* **6**(1–2), 79–90 (2021). <https://doi.org/10.1007/s41104-021-00075-4>
  15. Wang Z., Zhu Y., Tao C., Wang Q., Zhao M., Chen Z.: Effect of Engine Oil on Fuel Consumption and Durability of Heavy-Duty Vehicle. In: SAE-China (ed.) Proceedings of the 19th Asia Pacific Automotive Engineering Conference & SAE-China Congress 2017: Selected Papers. SAE-China 2017. Lecture Notes in Electrical Engineering, vol 486. Springer, Singapore (2017). [https://doi.org/10.1007/978-981-10-8506-2\\_33](https://doi.org/10.1007/978-981-10-8506-2_33)

**Publisher's Note** Springer Nature remains neutral with regard to jurisdictional claims in published maps and institutional affiliations.